




Wetting of grain boundary triple junctions by intermetallic delta-phase in the Cu–In alloys

Boris Straumal^{1,2,3,4,*} , Olga Kogtenkova², Marat Bulatov⁵, Alexei Nekrasov⁶, Alexandr Baranchikov⁷, Brigitte Baretzky¹, and Alexandr Straumal^{2,4}

¹Institute of Nanotechnology, Karlsruhe Institute of Technology, Hermann-von-Helmholtz-Platz 1, 76344 Eggenstein-Leopoldshafen, Germany

²Institute of Solid State Physics, Russian Academy of Sciences, Academician Ossipyan Street 2, Chernogolovka, Russia 142432

³Chernogolovka Scientific Center of Russian Academy of Sciences, Lesnaja Street 9, Chernogolovka, Russia 142432

⁴NUST MISiS, Leninskii Prospect 4, Moscow, Russia 119049

⁵Scientific and Technological Center of Unique Instrumentation, Russian Academy of Sciences, Butlerov Street 15, Moscow, Russia 117342

⁶Institute of Experimental Mineralogy, Russian Academy of Sciences, Academician Ossipyan Street 2, Chernogolovka, Russia 142432

⁷Kurnakov Institute of General and Inorganic Chemistry, Russian Academy of Sciences, Leninsky Prospect 31, Moscow, Russia 119991

Received: 16 August 2020

Accepted: 7 December 2020

Published online:
3 January 2021

© The Author(s), under exclusive licence to Springer Science+Business Media, LLC part of Springer Nature 2021

ABSTRACT

The paper studies the wetting of grain boundary triple junctions (GB TJs) by the second solid phase (intermetallic) δ in the Cu–In alloys. In this system, the portion of grain boundaries in a copper-based solid solution (Cu), which are “wetted” by the second solid phase δ , changes non-monotonically with increasing temperature. At first, the portion of such completely wetted GBs increases from zero to almost 100% when the sample is heated, and then quickly falls back to zero. The condition of complete wetting for the GB TJs ($\sigma_{GB} > 1.73 \sigma_{SS}$) is less stringent than for the GBs ($\sigma_{GB} > 2 \sigma_{SS}$). Therefore, if the transition from incomplete to complete wetting occurs with an increase in temperature, then all GB TJs should become completely wetted at a temperature T_{WTJ} , lower than the temperature T_{WGB} , at which all GBs become completely wetted. In this work on the Cu–In system, it was found experimentally for the first time that the wetting of the GB TJs also behaves non-monotonously. The percentage of wetted GB TJs also increases to 100% at first and then falls with increasing temperature. In this case, the portion of wetted GB TJs exceeds the portion of wetted GBs not only when it increases with increasing temperature, but also then, with the subsequent disappearance of fully wetted GBs.

Handling Editor: M. Grant Norton.

Address correspondence to E-mail: straumal@issp.ac.ru

Introduction

Phase transformations in solids are a tool in the hands of a materials scientist that allows her/him to control the structure of materials and change their properties in a directional way. Such phase transformations include, first of all, melting and solidification, formation and decomposition of a solid solution, amorphization, ordering and disordering, eutectic, peritectic, eutectoid and peritectoid transformations, allotropic phase transitions (for example, in titanium, iron, zirconium, manganese, etc.). However, in addition to transformations in three-dimensional phases, there are also phase transformations at the internal interfaces like grain boundaries (GBs) and interphase boundaries (IBs) [1]. First of all, they include the wetting phase transitions [2]. The melt can completely or partially wet the grain boundaries [3]. In the first case, the contact angle between the liquid and solid phases is zero, and the melt layer completely separates one grain from another [4]. In the second case, the liquid phase has the form of separate droplets with a nonzero contact angle along the contact line of the boundary and the liquid, and the melt does not completely substitute the interface [5]. The thin layers of a second phase can form in the grain boundaries in case of a deficit of wetting phase [6] or in case if the bulk second phase is not in the equilibrium [7]. Such thin layers are frequently called as GB complexions (see [8, 9] and references therein).

The transition from partial to complete wetting and back can occur when the temperature or pressure changes [3, 10]. First, Cahn, as well as Ebner and Saam, have shown theoretically that wetting transitions at the external or internal interface represent true two-dimensional phase transformations [11, 12]. Later, the prediction of Cahn was shown to be consistent with surface thermodynamics (adsorption equations of Butler and Gibbs), also being in agreement with experimental data [12–15]. The same idea was also extended to GBs [16]. Following these predictions, the wetting transitions were observed experimentally in numerous works (see for example [1, 10, 17, 18]). The wetting transitions can be either of the first or second order (continuous) [19, 20]. As we study the wetting phase transitions at the internal interface, new lines of these transformations increasingly enrich and complement the traditional phase diagrams for three-dimensional systems [17].

For example, in two-phase regions of bulk phase diagrams, where solid solution and melt are in equilibrium, the new tie-lines of GB wetting phase transitions steadily appear. Usually, these are two horizontal lines that limit the temperature range, in which gradually, one after the other, the GBs with different energy σ_{GB} become completely wetted [2, 21]. The lower of these tie-lines corresponds to the minimum wetting temperature T_{wmin} for the GBs with the highest energy σ_{GBmax} , and the upper one corresponds to the maximum wetting temperature T_{wmax} for the GBs with the lowest energy σ_{GBmin} . At the GBs, not only thick layers of the “true” bulk liquid phase can be formed, but also thin layers of specific grain-boundary phases. For example, the lines of grain-boundary phase transitions of pre-wetting and pre-melting depart into single-phase region of the solid solution from the intersection point of GB wetting tie-line with solidus line [5, 7].

In addition to bulk (three-dimensional) phases and two-dimensional boundaries of their separation in solids, there are also linear (or one-dimensional) defects. Together with well-known dislocations, they also include the lines of the triple junction of grain boundaries (GB TJs). It turns out that wetting phase transformations can also be observed on one-dimensional (linear) defects [22]. In the case of complete wetting, the linear defect is replaced by a second-phase channel along its entire length, and in the case of incomplete wetting, chains of second-phase particles are observed on the dislocation, which “adorn” it like beads [23]. Various possible combinations of completely and partially wetted GBs and GB TJs are schematically shown in Fig. 1. The wetting phase transformations on one-dimensional (linear) defects are even more difficult to observe than on two-dimensional ones. In the case of triple junctions of grain boundaries, the morphology of the wetting phase, in contrast to the dislocation, is more like a three-sided prism, with GBs at its vertices. The second phase, wetting the grain boundaries, can be either liquid or solid [24, 25]. The phenomena associated with the wetting of the GB by the second solid phase were observed in a variety of systems: aluminum-based alloys [26], titanium alloys [27], tungsten alloys [28], steels [29], superalloys [30], multicomponent alloys without the major component (so-called high-entropy one) [31], composites [32], welded and soldered joints [33]. The wetting of the GB by the second solid phase is called also GB spreading of a second solid phase.

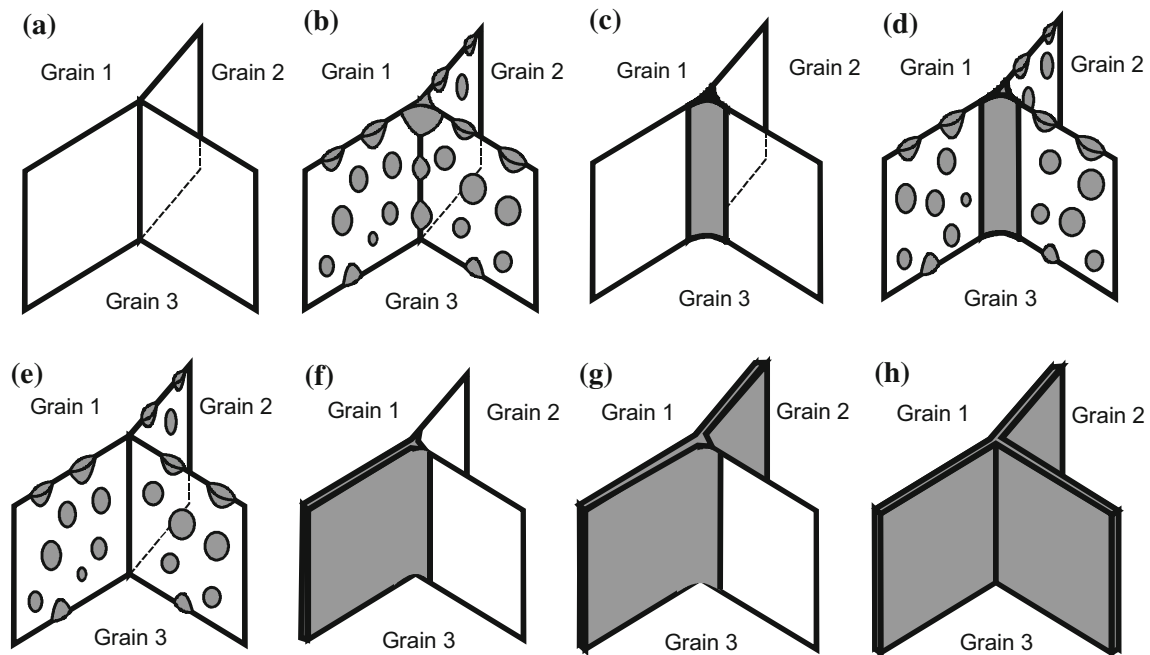


Figure 1 Triple junction (TJ) of grain boundaries (GBs) between grains 1, 2 and 3. **a** “Dry” TJ in contact with three dry GBs. **b** Partially wetted GB TJ in contact with three partially wetted GBs. **c** Completely wetted GB TJ in contact with three “dry” GBs. **d** Completely wetted GB TJ in contact with three partially wetted

GBs. **e** Dry GB TJ in contact with three partially wetted GBs. **f** Completely wetted GB TJ in contact with one fully wetted GB. **g** Completely wetted GB TJ in contact with two fully wetted GBs. **h** Completely wetted GB TJ in contact with two fully wetted GBs.

This term somehow softens the excessive similarity with wetting by the melt.

Already D. McLean mentioned that wetting of TJs should occur under more “soft” conditions than that of GBs [34]. Referring to the older work of Smith [35], McLean showed using a very simple calculation that GB is completely wetted if $\sigma_{GB} > 2 \sigma_{SL}$, and GB TJ is wetted if $\sigma_{GB} > \sqrt{3} \sigma_{SL}$ (here, σ_{SL} is the energy of the interphase boundaries of a solid and a liquid). This fact logically leads to a difference in the wetting transition temperature T_W for GBs (T_{WGB}) and GB TJs (T_{WTJ}). In [22], it was shown that the transition from incomplete to complete wetting of GB TJs occurs at a temperature T_{WTJ} which is lower than such a transition for the GBs themselves T_{WGB} . The question of the ratio of the wetting transition temperature for the grain boundaries T_{WGB} and their triple junctions T_{WTJ} for the “wetting” by the second solid phase remains, however, open. This work is devoted to the answer to this question.

In particular, when the melt wets GBs, the portion of fully wetted GBs always increases with increasing temperature [36, 37]. If the “wetting” phase is solid, then the portion of completely “wetted” GBs may, on

the contrary, fall with increasing temperature [38], or may behave non-monotonously (it initially increases, and then, starting from a certain temperature, falls again [18, 39]). These systems include Cu–In alloys, which we will study in this paper to understand how the portion of wetted triple junctions changes when the portion of wetted GBs behaves non-monotonically.

Materials and methods

In our work, copper alloys with indium concentrations of 4, 7.9, 12.5, 13.5, 17.5 and 22 wt% were studied. These alloys were manufactured using vacuum induction melting from highly pure components (99.9995 wt% Cu and 99.9993 wt% In). The resulting ingots with a diameter of 10 mm were cut into discs with a thickness of 2 mm, which after chemical polishing were sealed in evacuated quartz ampoules (with residual pressure of 4×10^{-4} Pa). These ampoules were then annealed in a muffle furnace at temperatures from 250 °C to 590 °C for 455–2120 h. The annealing temperatures and sample composition are marked on the Cu–In phase diagram (Fig. 2).

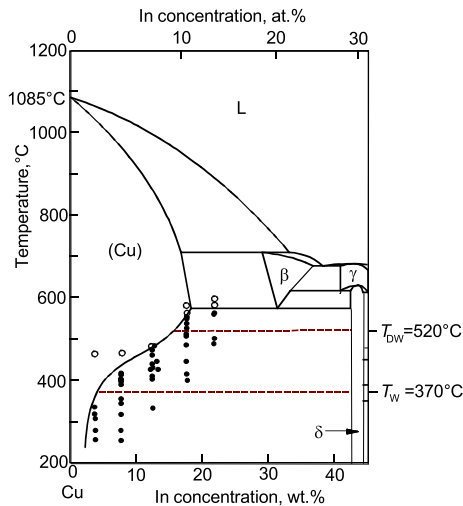


Figure 2 Part of the Cu–In phase diagram [40]. The filled points show the temperatures and concentrations at which annealing was performed in the two-phase region (Cu) + δ . Non-filled points indicate annealing conditions outside the two-phase region (Cu) + δ . Between tie-lines at $T_W = 370$ °C and $T_{DW} = 520$ °C (indicated by dotted lines) in Cu–In polycrystals, the GBs (Cu)/(Cu) are observed, completely “wetted” by continuous (spreaded) layers of the δ -phase [18].

After annealing, the samples were quenched in water, ground, polished and examined using scanning electron microscopy on a Tescan Vega NS5130MM device. Typical micrographs are shown in Fig. 3. Copper-based solid solution (Cu) looks dark in these micrographs, and intermetallic δ looks bright. The phase δ ($\text{Cu}_{70}\text{In}_{30}$) is present both in the volume of copper grains in the form of thin plates, and at the boundaries of copper grains. GBs in (Cu) were considered to be completely “wetted” if a thin layer of δ -phase completely separated the copper grains from each other throughout the boundary from one triple junction to the other. In the opposite case, the grain boundary was considered to be incompletely “wetted” by the δ -phase. The experiment was planned in such a way as to study the region near the solubility limit of indium in copper, where the volume fraction of the wetting phase is small. This is due to the fact that when the volume fraction of the wetting phase increases, the so-called apparent wetting occurs, when the second phase separates the grains of the first one simply because there is a lot of it, and not because the contact angle is zero [41].

The quantitative analysis of the GB TJ wetting transition was performed using the following criterion: each GB was considered fully wetted only when

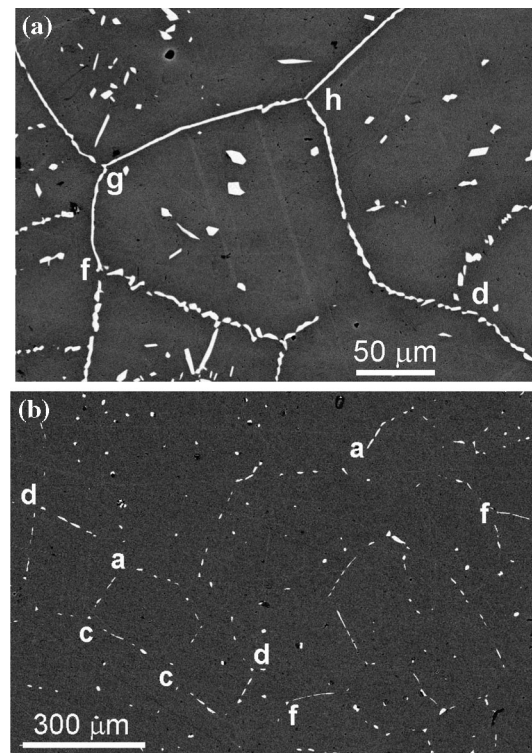


Figure 3 Microstructure of **a** Cu–12 wt% In alloy after annealing at 430 °C and **b** Cu– wt% In alloy annealed at 520 °C obtained by SEM (electron backscattering). The matrix (Cu) looks dark; the wetting layers of the δ -phase on the GBs and TJs look bright. Differently wetted GBs and TJs are marked with letters according to the scheme in Fig. 1.

the intermetallic layer covered the GB completely (all three GBs in Fig. 1h). If such a layer was interrupted, the GB was considered partially (incompletely) wetted (all three GBs in Fig. 1b, d, and e). If there was no second phase in the GB, it was considered dry (all three GBs in Fig. 1a). Similarly, the triple junction of the GB was considered wetted if the TJ contained a “star” of the second phase (Fig. 1c, d, f, g, h); in other cases, the TJ was considered “dry” (Fig. 1a, e). Careful sequential grinding of our annealed samples did not reveal any partially wetted TJ (shown in the diagram Fig. 1b). Therefore, they were not considered in the analysis. At least 500 GBs and/or GB TJs were analyzed at each temperature.

Results and discussion

Figure 3 shows two micrographs after annealing at temperatures of 430 °C and 520 °C. The first of them (Fig. 3a) clearly shows that the δ -phase spreaded

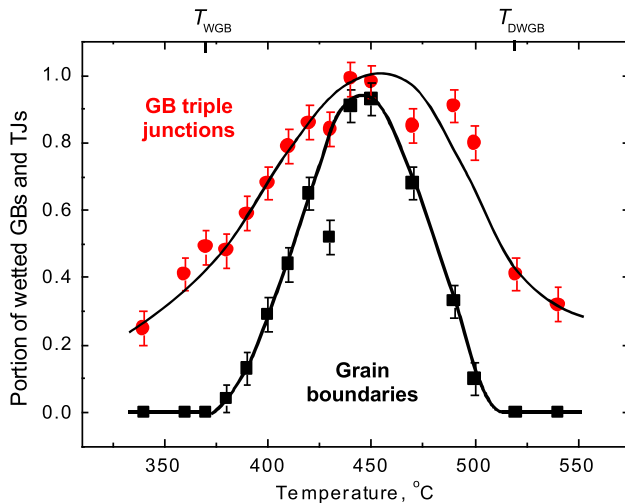


Figure 4 Temperature dependences of the portion of wetted grain boundaries (GBs) and triple junctions (TJs). Upper curve (filled circles) denotes the sum of configurations of wetted TJs shown in Fig. 1c, f, g, h. Lower curve (filled squares [18]): completely wetted GBs.

along most grain boundaries in (Cu) and completely separates the copper grains from each other. In other words, such grain boundaries in copper are completely “wetted” by the δ -phase. Figure 3b shows a micrograph in which almost all GBs in (Cu) contain chains of individual particles of the δ -phase. This means that such boundaries are incompletely “wetted” by the δ -phase. In [18], it was found that the portion of completely “wetted” GBs behaves non-monotonously with increasing temperature: at first, it increases, and, starting from a certain temperature, it falls again (the filled squares in Fig. 4). This means that when the temperature increases, there is a transition from incomplete “wetting” of the GBs in (Cu) by the δ -phase to complete one (i.e., to full GB spreading of δ -phase). With a further increase in temperature, the GBs in (Cu), completely “wetted” by the δ -phase, disappear again (Fig. 4). As a result, two new tie-lines appear in the (Cu) + δ area of copper–indium phase diagram (Fig. 2), namely at the temperature of GB wetting $T_{WGB} = 370$ °C and temperature of GB dewetting $T_{DWGB} = 520$ °C. Below, the first of these temperatures, there are no completely wetted GBs (see also Fig. 4, which shows the temperature dependence of the portion of completely wetted GBs and GB TJs). Above $T_{WGB} = 370$ °C, the first completely wetted (Cu) GBs appear in the samples, their portion increases with increasing temperature and reaches 93% (Fig. 4) [18]. At 440 °C, the

percentage of wetted GBs reaches a maximum of 93%. Then, with a further increase in temperature, the portion of completely wetted (Cu) GBs begins to fall. The percentage of wetted (Cu) GBs reaches zero again at $T_{DWGB} = 520$ °C. Above this temperature, the GBs completely wetted by the δ -phase are not observed in copper.

Various combinations of wetted GBs and TJs are marked in Fig. 3 with letters corresponding to the scheme in Fig. 1. The wetting phase at the grain boundaries is an intermetallic δ [18]. In Cu–In alloys, wetting of GBs with melt was also observed [41, 42]. Figure 4 shows the temperature dependence of the portion of wetted GBs and TJs. Filled circles (upper curve) indicate the portion of wetted TJs. It includes the sum of configurations shown in Fig. 1c, f, g, h. The percentage of wetted GB TJs (similar to that of fully wetted GBs) initially increases with increasing temperature: at 340 °C, it is $\sim 25\%$, and at $\sim 450 \pm 10$ °C, it reaches its maximum when all the GB triple junctions are wetted with the δ -phase. With a further increase in temperature, the percentage of wetted GB TJs begins to decrease, and at 540 °C it is only $\sim 32\%$. The filled squares (lower curve) show the portion of fully wetted GBs [18]. As we saw above, it also changes non-monotonously: first it grows, and then it falls with increasing temperature. Thus, the percentage of wetted GBs is everywhere less than the percentage of wetted GB triple junctions.

Consider the grain boundary in equilibrium contact with the second solid phase. The second solid phase can completely spread along the GB (or “wet” it) if $\sigma_{GB} > 2 \sigma_{SS}$, i.e., if the energy of the GB σ_{GB} is higher than the energy of the two interphase boundaries of (Cu) and δ solid phases $2 \sigma_{SS}$ (see the diagram in Fig. 5a, b). In the case of GB complete wetting in (Cu), it should be replaced by a layer of the second solid phase δ and two interphase boundaries of the “(Cu)/ δ ” (Fig. 5b). Let us now consider a triple junction (GB TJ) in the same alloy. The second solid phase δ can completely “wet” also a GB TJ. In this case, a triangular prism filled with the second solid phase δ replaces the (Cu) GB TJ (Fig. 5c, d). Then, a star of three (Cu) GBs (Fig. 5c) is replaced by a triangle of three interphase boundaries (Cu)/ δ (Fig. 5d). In the simplest case of an ideal symmetrical TJ with the same GBs having equal σ_{GB} , the condition for complete wetting is $\sigma_{GB} > \sqrt{3} \sigma_{SS}$. This condition is not as strict as for grain boundaries $\sigma_{GB} > 2 \sigma_{SS}$.

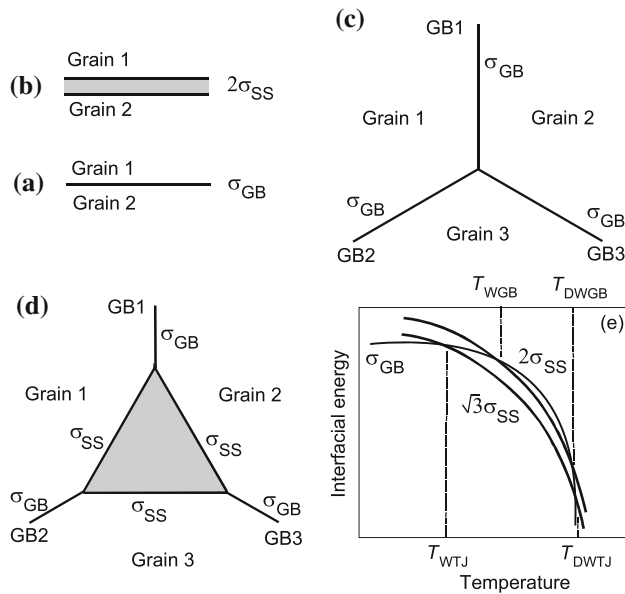


Figure 5 **a** “Dry” grain boundary with energy σ_{GB} . **b** Completely wetted GB, replaced by a layer second solid phase and two interfacial boundaries with energy $2\sigma_{SS}$. **c** “Dry” triple junction with GBs having the same energy σ_{GB} . **d** Triple junction of GBs, replaced by the triangle of the second solid phase (the case of complete wetting of the GB TJ). **e** Temperature dependence for the GB energy σ_{GB} , the energy $2\sigma_{SS}$ of two interphase boundaries of two solid phases when wetting GB and energy $\sqrt{3}\sigma_{SS}$ of interphase interfaces of two solid phases in the triangular prism substituting the completely wetted GB TJ.

Here, we consider only a case of a wetted TJ with macroscopic size (at least a few microns). Therefore, we neglect the energy of the GB TJ itself at the first approximation. Both σ_{GB} and σ_{SS} decrease with increasing temperature due to entropy reasons (Fig. 5e). If the temperature dependencies $\sigma_{GB}(T)$ and $2\sigma_{SS}(T)$ intersect at T_{WGB} , then a wetting phase transition occurs at T_{WGB} . Below T_{WGB} , the GB can co-exist in equilibrium contact with the second solid phase. Above T_{WGB} , the GB must be replaced by a layer of the second solid phase and cannot coexist in equilibrium contact with the second solid phase. The temperature dependence $\sqrt{3}\sigma_{SS}(T)$ lies lower than the dependence $2\sigma_{SS}(T)$ (Fig. 5e). Hence, $\sqrt{3}\sigma_{SS}(T)$ intersects with $\sigma_{GB}(T)$ at a temperature T_{WTJ} that is lower than T_{WGB} . As a result, fully wetted GBs are absent in the polycrystal in the temperature range between T_{WTJ} and T_{WGB} , but fully wetted TJ can exist below T_{WGB} and above T_{WTJ} .

In contrast to GB wetting with the liquid phase, if both phases are solid, the dependencies $\sigma_{GB}(T)$ and 2

$\sigma_{SS}(T)$ can intersect twice, at T_{WGB} and T_{DWGB} . In this case, above the T_{DWGB} (being the temperature of the second intersection of $\sigma_{GB}(T)$ and $\sqrt{3}\sigma_{SS}(T)$), the complete wetting (or spreading) of the GBs by the second solid phase disappears. Thus, GBs completely wetted by the second solid phase exist in the temperature range from T_{WGB} to T_{DWGB} . The dependencies $\sigma_{GB}(T)$ and $\sqrt{3}\sigma_{SS}(T)$ describing the wetting of triple junctions also intersect twice in this case. Such qualitative model is consistent with quantitative description in existing models on GB and s/s interfacial energies [43–46]. And, as follows from the diagram in Fig. 5e, the temperature of the first intersection of the dependencies $\sigma_{GB}(T)$ and $\sqrt{3}\sigma_{SS}(T)$ is lower than the temperature of the first intersection of the dependencies $\sigma_{GB}(T)$ and $2\sigma_{SS}(T)$. Conversely, the temperature of the second intersection of the dependencies $\sigma_{GB}(T)$ and $\sqrt{3}\sigma_{SS}(T)$ is higher than the temperature of the second intersection of the dependencies $\sigma_{GB}(T)$ and $2\sigma_{SS}(T)$. This means that the temperature range of existence of fully wetted GB triple junctions (from T_{WTJ} to T_{DWTJ}) is wider than the corresponding interval for fully wetted GBs (from T_{WGB} to T_{DWGB}), which we observe in the experiment (Fig. 4).

Indeed, such description is very simplified. Here, we completely ignore the fine structure of TJ itself as a one-dimensional lattice defect. However, the TJs—similar to GBs—can contain for example the linear complexions (like dislocations [47]). In this case, the “dry” portions of TJs between particles of a second phase (see Fig. 1a, b, e) are not really dry. We plan to study these phenomena more accurately in the future by using, for example, the X-rays or atomic force tomography [48].

Conclusions

Thus, in this work, it is experimentally confirmed that, if with increasing temperature there is a transition from incomplete “wetting” by the second solid phase to complete one for grain boundaries and their triple junctions, then all GB TJs become fully wetted at a temperature T_{WTJ} , lower than the temperature T_{WGB} , at which all GBs become completely wetted. If the wetting of GBs behaves non-monotonously with increasing temperature (that is, there is a reversed transition from incomplete wetting to complete

wetting), then the wetting of triple junctions also behaves non-monotonously. Namely, as the temperature increases, the portion of fully wetted triple junctions also falls. Moreover, the percentage of completely wetted GB TJs is always higher than that of completely wetted GBs.

Acknowledgements

The authors acknowledge the financial support of the state task of ISSP RAS, CSC RAS and IEM RAS. The SEM measurements were partially performed using shared experimental facilities supported by IGIC RAS state assignment.

Compliance with ethical standards

Conflict of interest There are no conflicts to declare.

References

- [1] Straumal BB, Zięba P, Gust W (2001) Grain boundary phase transitions and phase diagrams. *Intern J Inorgan Mater* 3:1113–1115. [https://doi.org/10.1016/S1466-6049\(01\)00108-8](https://doi.org/10.1016/S1466-6049(01)00108-8)
- [2] Rabkin EI, Shvindlerman LS, Straumal BB (1991) Grain boundaries: phase transitions and critical phenomena. *Int J Mod Phys B* 5:2989–3028. <https://doi.org/10.1142/S0217979291001176>
- [3] Chang LS, Rabkin E, Straumal B, Lejcek P, Hofmann S, Gust W (1997) Temperature dependence of the grain boundary segregation of Bi in Cu polycrystals. *Scripta Mater* 37:729–735. [https://doi.org/10.1016/S1359-6462\(97\)00171-1](https://doi.org/10.1016/S1359-6462(97)00171-1)
- [4] Noskovich OI, Rabkin EI, Semenov VN, Straumal BB, Shvindlerman LS (1991) Wetting and premelting phase transitions in 38°[100] tilt grain boundaries in (Fe–12at.%Si) Zn alloy in the vicinity of the A2–B2 bulk ordering in Fe–12at.%Si alloy. *Acta Metall Mater* 39:3091–3098. [https://doi.org/10.1016/0956-7151\(91\)90042-Y](https://doi.org/10.1016/0956-7151(91)90042-Y)
- [5] Straumal BB, Noskovich OI, Semenov VN, Shvindlerman LS, Gust W, Predel B (1992) Premelting transition on 38°<100> tilt grain boundaries in (Fe–10at.%Si)–Zn alloys. *Acta Metall Mater* 40:795–801. [https://doi.org/10.1016/0956-7151\(92\)90021-6](https://doi.org/10.1016/0956-7151(92)90021-6)
- [6] Chang LS, Rabkin E, Straumal BB, Hoffmann S, Baretzky B, Gust W (1998) Grain boundary segregation in the Cu–Bi system. *Def Diff Forum* 156:135–146. <https://doi.org/10.4028/www.scientific.net/DDF.156.135>
- [7] Chang LS, Straumal BB, Rabkin E, Gust W, Sommer F (1997) The solidus line of the Cu–Bi phase diagram. *J Phase Equil* 18:128–135. <https://doi.org/10.1007/s11669-006-5002-z>
- [8] Kaptay G (2012) Nano-Calphad: extension of the Calphad method to systems with nano-phases and complexions. *J Mater Sci* 47:8320–8335. <https://doi.org/10.1007/s10853-012-6772-9>
- [9] Goins PE, Frazier WE III (2020) A model of grain boundary complexion transitions and grain growth in Yttria-doped alumina. *Acta Mater* 188:79–91. <https://doi.org/10.1016/j.actamat.2019.12.061>
- [10] Straumal B, Rabkin E, Lojkowski W, Gust W, Shvindlerman LS (1997) Pressure influence on the grain boundary wetting phase transition in Fe–Si alloys. *Acta Mater* 45:1931–1940. [https://doi.org/10.1016/S1359-6454\(96\)00332-1](https://doi.org/10.1016/S1359-6454(96)00332-1)
- [11] Cahn JW (1977) Critical point wetting. *J Chem Phys* 66:3667–3672. <https://doi.org/10.1063/1.434402>
- [12] Ebner C, Saam W (1977) New phase-transition phenomena in thin argon films. *Phys Rev Lett* 38:1486–1488. <https://doi.org/10.1103/PhysRevLett.38.1486>
- [13] Kaptay G (2020) A coherent set of model equations for various surface and interface energies in systems with liquid and solid metals and alloys. *Adv Colloid Interface Sci* 283:102212. <https://doi.org/10.1016/j.cis.2020.102212>
- [14] Mekler C, Kaptay G (2008) Calculation of surface tension and surface phase transition line in binary Ga–Tl system. *Mater Sci Eng A* 495:65–69. <https://doi.org/10.1016/j.msea.2007.10.111>
- [15] Kaptay G (2005) A method to calculate equilibrium surface phase transition lines in monotectic systems. *Calphad* 29:56–67. <https://doi.org/10.1016/j.calphad.2005.04.004>
- [16] Kaptay G (2016) Modelling equilibrium grain boundary segregation, grain boundary energy and grain boundary segregation transition by the extended Butler equation. *J Mater Sci* 51:1738–1755. <https://doi.org/10.1007/s10853-015-9533-8>
- [17] Straumal BB, Baretzky B (2004) Grain boundary phase transitions and their influence on properties of polycrystals. *Interf Sci* 12:147–155. <https://doi.org/10.1023/B:INTJ.000028645.30358.f5>
- [18] Straumal BB, Kogtenkova OA, Kolesnikova KI, Straumal AB, Bulatov MF, Nekrasov AN (2014) Reversible “wetting” of grain boundaries by the second solid phase in the Cu–In system. *JETP Lett* 100:535–539. <https://doi.org/10.1134/S002136401420010>
- [19] Straumal BB, Gornakova AS, Kogtenkova OA, Protasova SG, Sursaeva VG, Baretzky B (2008) Continuous and discontinuous grain boundary wetting in the Zn–Al system.

- Phys Rev B 78:054202. <https://doi.org/10.1103/PhysRevB.78.054202>
- [20] Straumal BB, Gornakova AS, Sursaeva VG, Yashnikov VP (2009) Second-order faceting-roughening of the tilt grain boundary in zinc. *Int J Mater Res* 100:525–529. <https://doi.org/10.3139/146.110058>
- [21] Maksimova EL, Shvindlerman LS, Straumal BB (1988) Transformation of $\Sigma 17$ special tilt boundaries to general boundaries in tin. *Acta metall* 36:1573–1583. [https://doi.org/10.1016/0001-6160\(88\)90225-8](https://doi.org/10.1016/0001-6160(88)90225-8)
- [22] Straumal BB, Kogtenkova O, Zięba P (2008) Wetting transition of grain boundary triple junctions. *Acta Mater* 56:925–933. <https://doi.org/10.1016/j.actamat.2007.10.043>
- [23] Johnson E, Levinsen MT, Steenstrup S, Prokofjev S, Zhilin V, Dahmen U, Radetic T (2004) One-dimensional random walk of nanosized liquid Pb inclusions on dislocations in Al. *Phil Mag* 84:2663–2673. <https://doi.org/10.1080/14786430410001671412>
- [24] Gornakova AS, Straumal BB, Nekrasov AN, Kilmametov A, Afonikova NS (2018) Grain boundary wetting by a second solid phase in Ti–Fe alloys. *J Mater Eng Perform* 27:4989–4992. <https://doi.org/10.1007/s11665-018-3300-3>
- [25] Straumal BB, Kogtenkova OA, Straumal AB, Baretzky B (2018) Grain boundary wetting-related phase transformations in Al and Cu-based alloys. *Lett Mater* 8:364–371. <https://doi.org/10.22226/2410-3535-2018-3-364-371>
- [26] Liu L, Ren D, Liu F (2014) A review of dissimilar welding techniques for magnesium alloys to aluminum alloys. *Materials* 7:3735–3757. <https://doi.org/10.3390/ma7053735>
- [27] Chuvil'deev VN, Kopylov VI, Nokhrin AV, Tryaev PV, Tabachkova NY, Chegurov MK, Kozlova NA, Mikhaylov AS et al (2019) Effect of severe plastic deformation realized by rotary swaging on the mechanical properties and corrosion resistance of near- α -titanium alloy Ti-2.5Al-2.6Zr. *J Alloys Compd* 785:1233–1244. <https://doi.org/10.1016/j.jallcom.2019.01.268>
- [28] Ahangarkani M, Zangeneh-Madar K, Borji S, Valefi Z (2017) The effect of post-sintering annealing on the erosion resistance of infiltrated W-Cu composites. *Mater Lett* 209:566–570. <https://doi.org/10.1016/j.matlet.2017.08.057>
- [29] Tian JY, Xu G, Zhou MX, Hu HJ, Wan XL (2017) The effect of Cr and Al addition on transformation and properties in low-carbon bainitic steels. *Metals* 7:40. <https://doi.org/10.3390/met7020040>
- [30] Turner RP, Panwisawasa C, Lu Y, Dhiman I, Basoalto HC, Brooks JW (2018) Neutron tomography methods applied to a nickel-based superalloy additive manufacture build. *Mater Lett* 230:109–112. <https://doi.org/10.1016/j.matlet.2018.07.112>
- [31] Jodi DE, Park J, Park N (2019) Precipitate behavior in nitrogen-containing CoCrNi medium-entropy alloys. *Mater Charact* 157:109888. <https://doi.org/10.1016/j.matchar.2019.109888>
- [32] Krylova TA, Chumakov YuA (2020) Fabrication of Cr-Ti-C composite coating by non-vacuum electron beam cladding. *Mater Lett* 274:128022. <https://doi.org/10.1016/j.matlet.2020.128022>
- [33] Yao P, Li XY, Liang XB, Yu B, Jin FY, Li Y (2017) A study on interfacial phase evolution during Cu/Sn/Cu soldering with a micro interconnected height. *Mater Charact* 131:49–63. <https://doi.org/10.1016/j.matchar.2017.06.033>
- [34] McLean D (1957) Grain boundaries in metals. Clarendon Press, Oxford, p 95
- [35] Smith CB (1948) Introduction to grains, phases, and interfaces—an interpretation of microstructure. *Trans AIMME* 175:15–51. <https://doi.org/10.1007/s11661-010-0215-5>
- [36] Straumal B, Gust W, Molodov D (1995) Wetting transition on the grain boundaries in Al contacting with Sn-rich melt. *Interface Sci* 3:127–132. <https://doi.org/10.1007/BF00207014>
- [37] Straumal BB, Gust W, Watanabe T (1999) Tie lines of the grain boundary wetting phase transition in the Zn-rich part of the Zn–Sn phase diagram. *Mater Sci Forum* 294:411–414. <https://doi.org/10.4028/www.scientific.net/MSF.294-296.411>
- [38] Protasova SG, Kogtenkova OA, Straumal BB, Zięba P, Baretzky B (2011) Inversed solid-phase grain boundary wetting in the Al–Zn system. *J Mater Sci* 46:4349–4353. <https://doi.org/10.1007/s10853-011-5322-1>
- [39] Straumal BB, Kogtenkova OA, Straumal AB, Kuchyeyev YuO, Baretzky B (2010) Contact angles by the solid-phase grain boundary wetting in the Co–Cu system. *J Mater Sci* 45:4271–4275. <https://doi.org/10.1007/s10853-010-4377-8>
- [40] Massalski TB et al (eds) (1993) Binary alloy phase diagrams. ASM International, Materials Park
- [41] Straumal AB, Bokstein BS, Petelin AL, Straumal BB, Baretzky B, Rodin AO, Nekrasov AN (2012) Apparently complete grain boundary wetting in Cu–In alloys. *J Mater Sci* 47:8336–8343. <https://doi.org/10.1007/s10853-012-6773-8>
- [42] Straumal AB, Yardley VA, Straumal BB, Rodin AO (2015) Influence of the grain boundary character on the temperature of transition to complete wetting in Cu–In system. *J Mater Sci* 50:4762–4771. <https://doi.org/10.1007/s10853-015-9025-x>
- [43] Kaptay G, Barczy T (2005) On the asymmetrical dependence of the threshold pressure of infiltration on the wettability of the porous solid by the infiltrating liquid. *J Mater Sci* 40:2531–2535. <https://doi.org/10.1007/s10853-005-1987-7>

- [44] Weltsch Z, Lovas A, Takács J, Cziráki Á, Toth A, Kaptay G (2013) Measurement and modelling of the wettability of graphite by a silver-tin (Ag-Sn) liquid alloy. *Appl Surf Sci* 268:52–60. <https://doi.org/10.1016/j.apsusc.2012.11.150>
- [45] Baumli P, Sytchev J, Kaptay G (2010) Perfect wettability of carbon by liquid aluminum achieved by a multifunctional flux. *J Mater Sci* 45:5177–5190. <https://doi.org/10.1007/s10853-010-4555-8>
- [46] Rohrer GS (2011) Grain boundary energy anisotropy: a review. *J Mater Sci* 46:5881–5895. <https://doi.org/10.1007/s10853-011-5677-3>
- [47] Kuzmina M, Herbig M, Ponge D, Sandlöbes S, Raabe D (2015) Linear complexions: confined chemical and structural states at dislocations. *Science* 349:1080–1083. <https://doi.org/10.1126/science.aab2633>
- [48] Mazilkin AA, Straumal BB, Kilmametov AR, Boll T, Baretzky B, Kogtenkova OA, Korneva A, Zięba P (2019) Competition for impurity atoms between defects and solid solution during high pressure torsion. *Scripta Mater* 173:46–50. <https://doi.org/10.1016/j.scriptamat.2019.08.001>

Publisher's Note Springer Nature remains neutral with regard to jurisdictional claims in published maps and institutional affiliations.